Thin Receiver Freeform Lenslet Concentrator Array for LiFi

Janis Sperga
pureLiFi Ltd
Edinburgh EH6 6QH, U.K.
Email: janis.sperga@purelifi.com

Rui Bian
pureLiFi Ltd
Edinburgh EH6 6QH, U.K.

Mohamed Sufyan Islim
pureLiFi Ltd
Edinburgh EH6 6QH, U.K.

John Kosman
pureLiFi Ltd
Edinburgh EH6 6QH, U.K.

Giovanni Luca Martena
pureLiFi Ltd
Edinburgh EH6 6QH, U.K.

Eoin Murphy
pureLiFi Ltd
Edinburgh EH6 6QH, U.K.

Harald Haas
pureLiFi Ltd
Edinburgh EH6 6QH, U.K.
Email: harald.haas@purelifi.com

***Abstract*—Emerging optical wireless communication (OWC) and LiFi require an ever-increasing bandwidth and decreasing size of the receiver modules compatible with mobile communication. This leads to using arrayed photodetector (PD) solutions for the receiver. However, the classical imaging solutions (e.g., convex lenses) struggle to achieve the required optical concentration at mobile form factors. In comparison, the non-imaging solutions (e.g., compound parabolic concentrators (CPCs)) provide poor uniformity of the irradiance distribution at the PD plane that can impair the link performance in the arrayed PD receivers.**

This paper proposes a novel approach using a freeform lenslet concentrator array to achieve an enhanced gain at a 5-degree field-of-view (FoV) compared to existing standard imaging optics solutions. The design also maintains a better irradiance uniformity and smaller refracted beam angle than the non-imaging solutions. Making it a promising optical solution that can help bridge the gap between imaging and non-imaging optics for high bandwidth arrayed PD receivers for mobile LiFi and OWC applications.

***Index Terms*—Freeform optics, receiver optics, freeform lenslet array, arrayed receiver, LiFi, optical wireless communication (OWC).**

I. Introduction

The importance of optical front-end (OFE) in optical wireless communication (OWC) and LiFi cannot be overstated. Integrating LiFi modules in mobile devices demands ever smaller optical front-end elements, including concentrators [1]. This limits the size of the concentrators and photodetectors (PDs) to a few millimeters in modules intended for mobile applications.

The increasing requirement for high-bandwidth applications necessitates using a PD array for receiver modules that can maintain both the high bandwidth and signal strength [2]. In turn, using PD arrays in mobile communications requires concentrating optics to generate the necessary optical gain for a given field-of-view (FoV) with as uniform irradiance distribution as possible to minimize the losses due to the limited fill factor of the PDs of the array with such problems already being noted in the solar concentration applications [3].

Previously for point-to-point (P2P) communication, standard imaging optics consisting, for example, of convex lenses were frequently used in the OWC experiments [4]. However, while being capable of achieving a large gain and uniform irradiance distribution, receivers equipped with conventional imaging optics are severely limited in their FoV and suffer significantly from link misalignment [5]. One of the common solutions to address the FoV limitation is to use the lens in the de-focused mode, where the array plane is placed before the focal plane of the lens [6]. The trade-off in this regime is decreased gain for enhanced FoV.

Alternatively, non-imaging optics have been frequently used as concentrators in OWC receivers [7]. In general, non-imaging optics can be designed to be more robust against link misalignment, providing high enough optical gain for comparably larger FoV than that is achievable in imaging optics [7]. Theoretically, the optical gain for the desired FoV in non-imaging optics is only limited by the Etendue conservation [8].

A notable example of non-imaging optics is compound parabolic concentrators (CPCs) which are among the more popular choices for receiver optics in LiFi and OWC [7]. However, a significant factor limiting the CPC implementation in mobile communication is the optical gain dependency on the height of the CPC for a given FoV [9]. This often can lead to the required CPC size exceeding the permissible form factor of the receiver module. One way to reduce the height of the CPC while retaining the FoV, exit aperture size and gain is to modify the concentrator into a dielectric, totally internally reflecting concentrator (DTIRC) [10]. While DTIRCs can be designed for mobile communications, they would posses a similar drawback of the CPCs - the non-uniform irradiance distribution (transmission angle curves) at the PD plane [9].

As already mentioned, while the impact of non-uniformity is relatively minor in a single PD receiver link, it can negatively impact performance when a PD array is considered. A way to work around this problem would involve using an array of micro CPCs where an exit aperture of each CPC would match the photoactive area of a single array PD [11]. While such an approach is promising, the main limitation would be developing such concentrators for micrometer scale apertures.

Recently freeform optics have emerged as a potentially viable solution in OWC and LiFi. Initially finding their inception in solar concentration applications [12], freeform optics have found their way into OWC with research topics that cover transmitter beam shaping, freeform compound concentrators, and freeform diversity receivers [13]–[15]. To the best of our knowledge, so far studies of freeform optics design for limited-size factor mobile communications have been limited.

This work presents a novel thin freeform lenslet array concentrator for the LiFi receiver module. We compare our design's performance in terms of gain and generated photocurrent for various PD size arrays to conventional imaging optics (convex lens) and non-imaging optics (CPC).

The rest of the paper is organized as follows: section II describes the freeform lenslet array design. In section III, the optical setup is described for the simulations. Section IV evaluates and compares the design to conventional imaging and non-imaging optics. The paper is concluded in section V.

II. Freeform Lenslet Array Design

In this section, we propose a freeform lenslet array concentrator design consisting of a larger single primary optical lenslet (POL) located at the array's center, and multiple secondary optical lenslets (SOL).

A. Freeform Lenslet Array Design

The main design idea is illustrated in Fig.1 here, the array consists of SOLs made up of freeform prisms located at the outer perimeter of the array and a POL, which is a convex-shaped lens in the center of the array. The central POL achieves most of the optical gain, while the side SOLs enhance FOV by redirecting oblique incident rays to the POL and providing additional concentration from the edges. Each lenslet is calculated by solving a linear assignment problem (LAP) for the Monge-Kantorovich mass transportation problem (MTP) based on the algorithm from [16] in MATLAB. The freeform

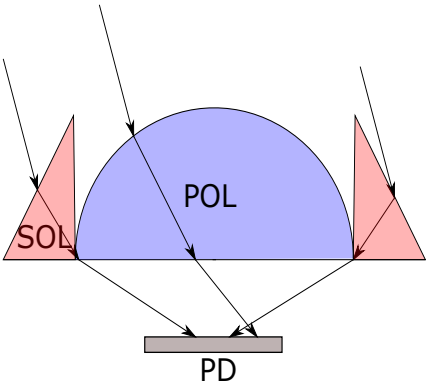

Fig. 1: Diagram of side-view of freeform lenslet array design for limited size factor imaging concentration. POL denotes primary optical lenslet, while SOL denotes secondary optical lenslet. PD denotes photodetector.

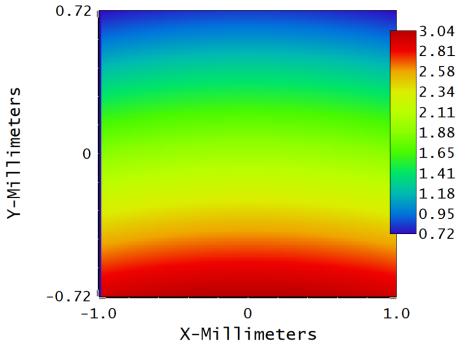

Fig. 2: The sag distribution of a SOL, the colorscale is given in mm.

surface is then optimised using Zemax Optic studio to achieve the best gain performance for a given FoV.

In this paper, we consider a scenario for a limited form factor mobile device module where the total height from the sag of the POL to the surface of the photodetector (PD) is limited to 5 mm. The width of the lenslet array is set to 8 mm, to accommodate the typical size of a smartphone sensor of around 1 cm. Each SOL has been designed to have a slightly convex curved outer surface to focus light and enhance the optical concentration of the array. A sag distribution of an SOL is shown in Fig.2. There are 12 SOLs and 1 POL in the freeform lenslet array. Each SOL is designed to be $2 \times 1.72\,\mathrm{mm}^2$ sized ranging from 3.04 mm in height at sides and 3.32 mm at the edges. The POL is $3 \times 3\,\mathrm{mm}^2$ size and 3.4 mm height. The resulting freeform lenslet array is shown in Fig.3.

The ray diagram of the design at a normal incidence is shown in Fig.4. As expected, the POL acts as a standard convex lens focusing light on its focal plane. At the same time, SOLs redirect and focus the incident at their surface rays towards the central axis of the array, enhancing the optical gain. The focal point is located about 3 mm away from the input aperture. Even though the POL is a spherical convex

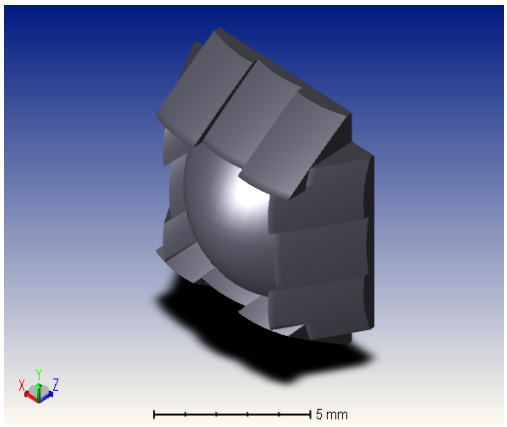

Fig. 3: Freeform lenslet array in isotropic projection.

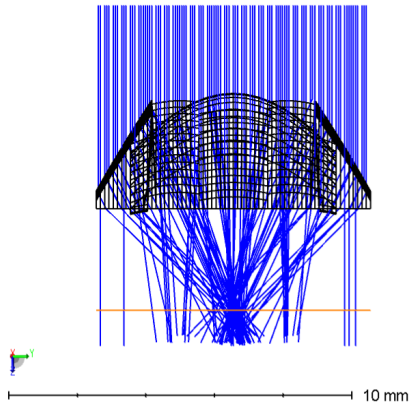

Fig. 4: Ray diagram of the lenslet array.

lens shape, the spot at the focal plane has a more extensive point spread than for a standard convex lens. This is due to slightly different focal lengths of SOLs, and various optical path lengths are taken by the rays propagating through SOLs and POL.

The target PD area was set to $1 \times 1\,\mathrm{mm}^2$. The distance from the exit aperture of the array to the PD was determined to be 1.5 mm. The FoV for these dimensions was around 5 degrees (the FoV is defined for the angle where optical gains drop below 90% of max gain at normal incidence). For the design, the material of choice was poly-carbonate.

For this size factor array, the diameter of the lenslet array is larger than the distance towards the PD; therefore, the light collection happens before the focal plane of the array. Thus, for the receiver performance with the lenslet array, susceptibility towards the spot wander decreases, allowing for broader FoV than in a focused scenario. At the same time, the SOLs partially compensate for the gain loss due to the de-focusing.

III. Optical Test Setup

In this section we will describe the optical test setup used for the ray-tracing simulations.

A. Simulation Parameters

We assume a 10 mW optical output power infrared $\lambda = 850\,\mathrm{nm}$ wavelength vertical cavity surface emitting laser (VCSEL) source for the transmitter end. The receiver is located at $1\,m$ distance from the transmitter. The incident power at the receiver input aperture of $8 \times 8\,\mathrm{mm}^2$ is calculated to be $1.54 \times 10^{-5}\,\mathrm{W}$. The ray-tracing simulation is performed with 10^7 rays. We assume no background illumination.

B. Size parameters of imaging and non-imaging optical elements

In this subsection, we will describe the size parameters for standard imaging (convex lens) and non-imaging (CPC) optical devices that we will use to compare with the freeform lenslet design.

For the convex lens, we set the thickness to 3.4 mm and diameter to 8 mm to match the freeform lenslet array dimensions; the PD plane is placed 1.5 mm away from the exit aperture of the lens. For these dimensions, the focal length of a standard convex lens is 3 mm; therefore, in these ray tracing simulations, the lens is de-focused. In the case of CPC, we put the PD plane at the exit aperture. The height of the CPC is then set to 4.9 mm and the acceptance angle to 5 degrees.

C. PD Array Structure

As discussed in the previous sections, this work aims to analyse and compare the freeform lenslet array's optical performance to the traditional imaging and non-imaging solutions for a PD array receiver. To this end we tested $1 \times 1\mathrm{mm}^2$ PD arrays with $25 \times 25\,\mu\mathrm{m}^2$, $50 \times 50\,\mu\mathrm{m}^2$,$100 \times 100\,\mu\mathrm{m}^2$ and $200 \times 200\,\mu\mathrm{m}^2$ sized photodetector elements. We assume the array's lattice constant (spacing between two PD elements) to be half of the PD element width.

To evaluate the photocurrent generated by the PD array, we assume that each PD element is a Si avalanche photodiode (APD). For reference, we will use the responsivity characteristics of Hamamatsu S12023-02 Si APD [17] with a responsivity of 52 A/W at 850 nm including gain. We note that any other small-size photodiode could be used instead. Furthermore, while the reference APD size is $200 \times 200\,\mu\mathrm{m}^2$, we will assume the same responsivity for the smaller-sized APD arrays.

IV. Optical Design Performance

In this section, we will evaluate the performance of the freeform lenslet array in terms of achievable gain and generated APD array photocurrent vs angle of incidence. We will compare the design to the CPC and a convex lens.

A. Irradiance distribution from the array

The irradiance distributions at the $25 \times 25\,\mu\mathrm{m}^2$ sized APD array for the receiver with a freeform lenslet array at a normal uniform incidence and 5-degree incidence angle are shown in Figs.5a and 5b. One can observe that the addition of tilt only offsets the beam spot located along the lateral coordinates of the array without significantly affecting the uniformity and size of the beam spot. As expected, the freeform lenslet array acts as an optical imaging device.

The same beam offset can be observed for the convex lens at a 5-degree incidence angle, shown in Fig.6. Here, however, the beam spot size is considerably smaller and the collection efficiency of the light lower than in the freeform lenslet array case. Therefore, the freeform lenslet array at a short concentration distance for the same thickness and diameter provides a better light collection efficiency than conventional imaging optics of the same size. This is also reflected in the generated photocurrent of the array (sum of all the array APD contributions). Here the freeform lenslet array generates $16.78\,\mu\mathrm{A}$ compared to $9.27\,\mu\mathrm{A}$ generated by a convex lens at a 5-degree incidence.

The irradiance distribution at the $25 \times 25\,\mu\mathrm{m}^2$ sized APD array located at the exit aperture of a CPC at a 5-degree incidence angle is shown in Fig. 7. As expected, a CPC produces a

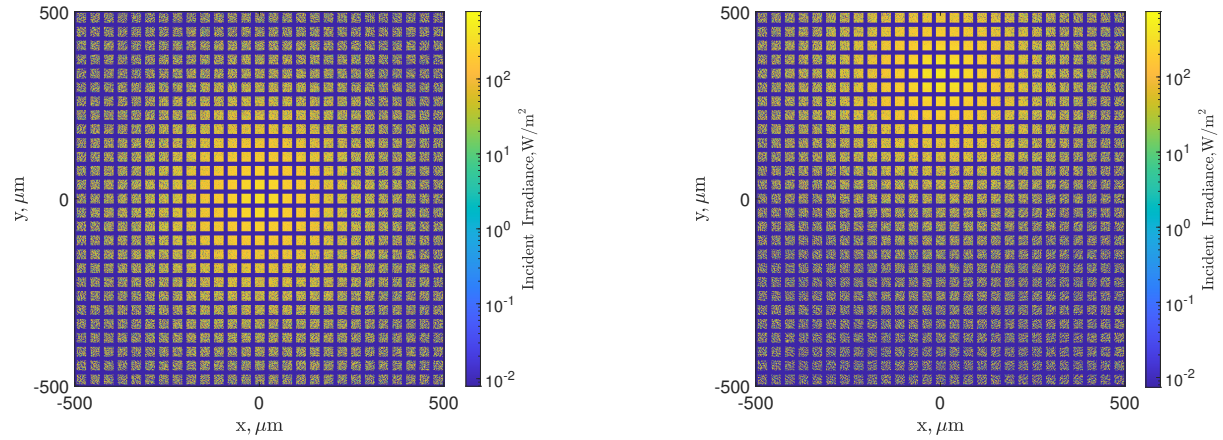

(a) (b)

Fig. 5: Irradiance distribution at the $25 \times 25\,\mu\mathrm{m}^2$ sized APD array for receiver with freeform lenslet array at a) normal incidence, b) 5 degree tilt along X axis. Each square represents an APD.

characteristic non-uniform irradiance distribution at an oblique incidence with a pronounced hotspot. The recovered optical power recovered for the CPC case is considerably larger than from a freeform lenslet array, with the generated APD array photocurrent reaching $28.89\,\mu$A at a 5-degree incidence angle.

B. Gain vs incidence angle

In this subsection, we will compare the optical gain between freeform lens array, de-focused convex lens and CPC at various incidence angles. Firstly, we will estimate the ideal optical gain - the gain for a case of a non-arrayed PD where the whole PD plane is a photoactive area. We define the optical gain as:

$$C = \frac{P_{\mathrm{opt}}}{P_{\mathrm{ref}}}; \tag{1}$$

Here P_{opt} - the total optical power recovered from the PD with an optical device (CPC, freeform lenslet array, de-focused lens) in front of it and P_{ref} - the power recovered at the PD without any optics.

A gains comparison is shown in Fig.8. As expected, the CPC performs the best for the same FoV as the freeform lenslet array, while the convex lens produces the worst performance of the three. It can be observed that the gains, when compared to each other roughly follow a ratio of 2.

C. Output photocurrent of the APD array vs incidence angle

This subsection compares the output photocurrent generated from the APD array between the considered optical concentrators. The output photocurrent is determined for different incidence angles between -5 and 5 degrees for different-size

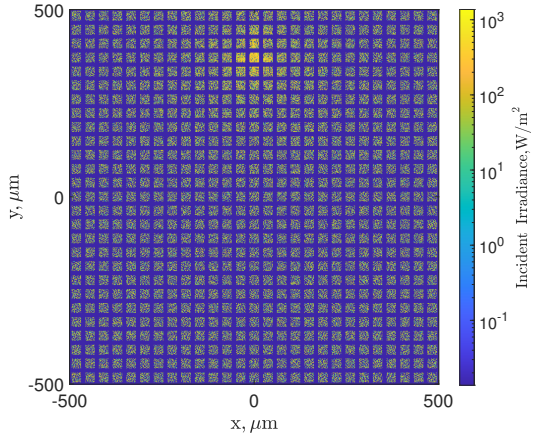

Fig. 6: Irradiance distribution at the $25 \times 25\,\mu\mathrm{m}^2$ sized APD array for receiver with convex lens at 5 degree incidence angle.

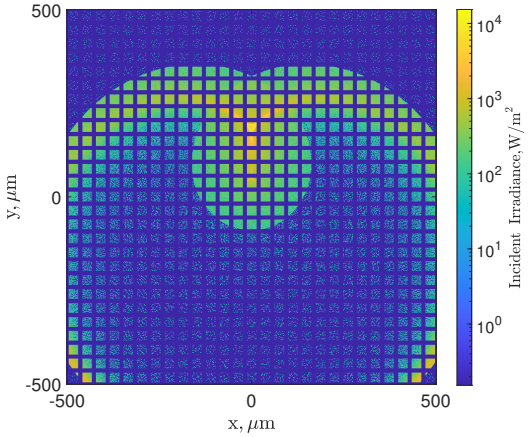

Fig. 7: Irradiance distribution at the $25 \times 25\,\mu\mathrm{m}^2$ sized APD array for receiver with CPC at 5 degree incidence angle.

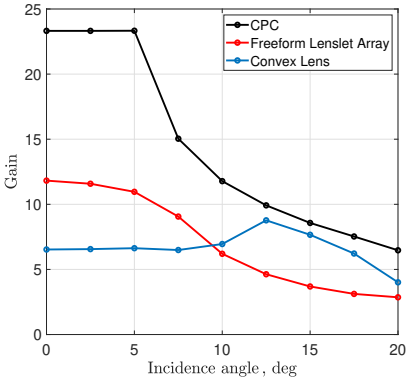

Fig. 8: Gain comparison between different receiver optics.

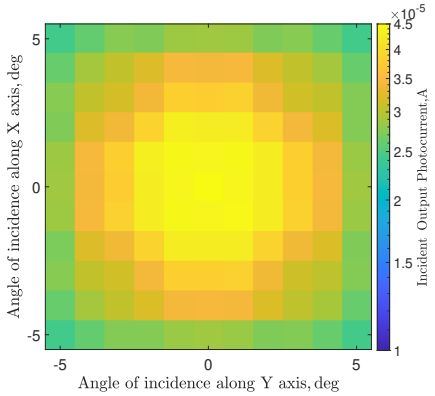

Fig. 10: Photocurrent dependency on the angle of incidence along X and Y axis generated by the $25 \times 25\,\mu\mathrm{m}^2$ sized APD array for receiver with CPC.

APD arrays by the expression [4]:

$$I_{\text{out}} = R_{\text{Rx}} \iint_A I(x, y)\, dx\, dy; \tag{2}$$

Here $R_{\text{Rx}} = 52\,\text{A/W}$ - Si APD responsivity, I - incidence irradiance (W/m^2) and A - the receiver plane area integration domain.

Fig.9 shows the output current from a $25 \times 25\,\mu\text{m}^2$ sized APD array with a freeform lenslet array at different incidence angles. As can be seen from the figure, the optical photocurrent remains stable at various incidence angles decreasing from $18.5\,\mu$A at normal incidence to $16.8\,\mu$A at 5 degree incidence angle along a single axis. The decrease is 9.2% within the defined FoV 10% decrease margins. Furthermore, for the 7 degree incidence case (the incident beam tilted by 5 degrees along both axes), the output array photocurrent drop is only 15.2% providing $15.7\,\mu$A. The same is observation can be done for $50 \times 50\,\mu\text{m}^2$, $100 \times 100\,\mu\text{m}^2$ and $200 \times 200\,\mu\text{m}^2$ sized APD array cases.

In comparison, for the same size APD array with a CPC for the concentrator, the output current dependency on the incidence angle is shown in Fig.10. As expected, the CPC achieves a much higher output photocurrent with peak $45.5\,\mu$A, at a normal incidence. However, the photocurrent variance is significantly higher than for a freeform lens. Furthermore, the drop in optical photocurrent is considerably more significant than in the freeform lenslet array case. Here at 5 degree incidence, the photocurrent decreases to $28.76\,\mu$A - a decrease of 36.8%. Already at a 2 degree incidence angle, the optical photocurrent has decreased by 7.7%. Therefore, effectively the FoV of the CPC has decreased by about half compared to the initial specification. This is contrary to the expected stable gain until the acceptance angle of the CPC is at 5 degrees incidence angle. The deterioration in performance can be primarily attributed to the non-uniform beam irradiance distribution incident on the array of APDs.

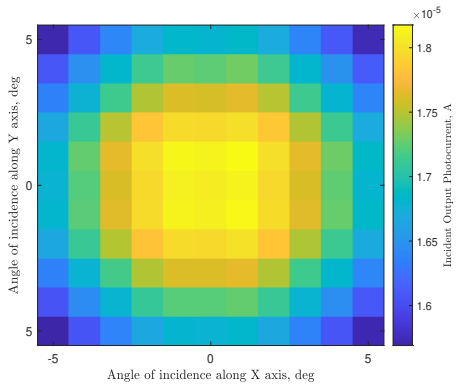

Fig. 9: Photocurrent dependency on the angle of incidence along X and Y axis generated by the $25 \times 25\,\mu\text{m}^2$ sized APD array for receiver with freeform lenslet array.

Thus, while the receivers with a CPC solution can provide robustness against the misalignment in the single PD OWC links, the application of CPCs for arrayed PD receivers is significantly more susceptible to the misalignment. The misalignment issues have to be considered in the design, which limits the usefulness of the CPC solution for high data throughput OWC and LiFi links. We observe the same FoV shrinkage and the non-uniform photocurrent output in the rest of the PD array sizes.

Fig.11 shows the mean output photocurrent averaged over different incidence angles for different array APD element sizes. We see that for any APD element-sized array, the CPC solution produces a higher output photocurrent than a freeform lenslet array. However, as seen from the error bars, the variance is also higher than for the freeform lenslet array for any sized array in the interval between 25μm and 200μm PDs. This is also reflected in the relative standard deviation of the output photocurrent (standard deviation divided by mean output photocurrent). For the CPC, the relative standard deviation ranges between 5% and 10% for the different-sized PD arrays, while for the freeform lenslet array, the range is between 0.1% and 0.2%.

Finally, so far, we have only considered the irradiance of distribution of the optical concentrators, but radiance also plays

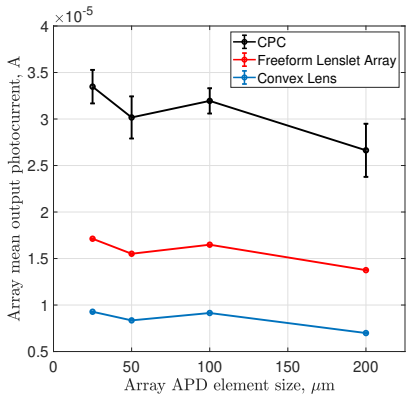

Fig. 11: Mean array output photocurrent vs array APD element size for different receiver optics.

an essential role in the optical concentration. We calculate the mean incidence angle at the APD array in the freeform lenslet array case to be 19 degrees and about 60 degrees for the CPC case. Due to the Fresnel reflections at the interface, an average of up to 50% (assuming cosine dependency of the responsivity of a PD on the incidence angle) of the concentrated light will be reflected in the CPC case. Only 8% is reflected in the freeform lenslet case. Therefore, the optical gain advantage of the CPC is minimised over the freeform lenslet array. While the Fresnel reflection coefficients can be decreased by the use of index-matching materials and anti-reflective (AR) coatings, a considerable amount of complexity and cost to the optical design is added in the process. The use of more optical elements adds towards the already existing complexity of placing a micro-sized PD array at the small exit aperture of CPC.

V. Conclusion

The proposed thin novel freeform lenslet array provides multiple advantages to the existing optical concentrators, particularly for the arrayed PD receivers. For limited mobile module form factors, the lenslet array is able to achieve larger gain with the same FoV and comparable uniformity to the standard imaging optics (e.g., convex lens). This makes the design viable for the high bandwidth mobile OWC and LiFi applications.

While the lenslet array achieves a smaller optical concentration than a non-imaging CPC solution, the higher uniformity of the irradiance distribution yields its benefits in a more stable photocurrent output at various incidence angles within the specified FoV. The significantly smaller incidence angle of the refracted beams (< 20 deg) at the PD array surface allows for a more straightforward optical design compared to the non-imaging optics case. There, the high angle (≥ 60 deg) AR coating and index matching materials are required to maintain the expected performance. This makes, in practice, the freeform lenslet array solution less complex and cheaper to manufacture for the arrayed PD receivers than a classical CPC.

However, further work is necessary to compare the performance of the lenslet array to other non-imaging optical concentrators, e.g., DTIRC, and other imaging optical solutions like micro-lenses and metalenses. Furthermore, the current design is limited in the achievable FoV, and the trade-offs between dimensions of the array, FoV and gain are to be further investigated.

Acknowledgment

The authors acknowledge the ENLIGHT'EM project (H2020-MSCA ITN-2018 n. 814215) for the fundamental support in this research.

References

[1] H. Burchardt, N. Serafimovski, D. Tsonev, S. Videv and H. Haas, "VLC: Beyond point-to-point communication," *IEEE Communications Magazine*, vol. 52, no. 7, pp. 98-105, July 2014.

[2] T. Koonen, "Indoor Optical Wireless Systems: Technology, Trends, and Applications," *Journal of Lightwave Technology*, vol. 36, no. 8, pp. 1459–1467, Apr. 2018, doi: 10.1109/jlt.2017.2787614.

[3] S. Hatwaambo, H. Hakansson, J. Nilsson, and B. Karlsson, "Angular characterization of low concentrating PV–CPC using low-cost reflectors," *Solar Energy Materials and Solar Cells*, vol. 92, no. 11, pp. 1347–1351, Nov. 2008, doi: 10.1016/j.solmat.2008.05.008.

[4] Z. Ghassemlooy, W. Popoola, and S. Rajbhandari, *Optical Wireless Communications: System and Channel Modelling with MATLAB*, 1st ed. USA: CRC Press, Inc., 2012.

[5] R. Mulyawan et al., "A comparative study of optical concentrators for visible light communications," *SPIE Proceedings*, Jan. 2017, doi: 10.1117/12.2252355.

[6] T. Koonen, K. A. Mekonnen, Z. Cao, F. Huijskens, N. Q. Pham, and E. Tangdiongga, "Beam-Steered Optical Wireless Communication for Industry 4.0," *IEEE Journal of Selected Topics in Quantum Electronics*, vol. 27, no. 6, pp. 1–10, Nov. 2021, doi: 10.1109/jstqe.2021.3092837.

[7] J. M. Kahn and J. R. Barry, "Wireless infrared communications," in *Proceedings of the IEEE*, vol. 85, no. 2, pp. 265-298, Feb. 1997, doi: 10.1109/5.554222.

[8] G. Smestad, H. Ries, R. Winston, and E. Yablonovitch, "The thermodynamic limits of light concentrators," *Solar Energy Materials*, vol. 21, no. 2, pp. 99–111, Dec. 1990, doi: 10.1016/0165-1633(90)90047-5.

[9] R. Winston, J. C. Minano, P. G. Benitez, and J. C. Bortz, *Nonimaging Optics*. Elsevier, 2005.

[10] X. Ning, R. Winston, and J. O'Gallagher, "Dielectric totally internally reflecting concentrators," Applied Optics, vol. 26, no. 2, p. 300, Jan. 1987, doi: 10.1364/ao.26.000300.

[11] H.-J. Choi et al., "Manufacturing of Compound Parabolic Concentrator Devices Using an Ultra-fine Planing Method for Enhancing Efficiency of a Solar Cell," *International Journal of Precision Engineering and Manufacturing-Green Technology*, vol. 8, no. 5, pp. 1405–1414, Dec. 2020, doi: 10.1007/s40684-020-00287-3.

[12] J. C. Miñano, P. Benítez, P. Zamora, M. Buljan, R. Mohedano, and A. Santamaría, "Free-form optics for Fresnel-lens-based photovoltaic concentrators," *Optics Express*, vol. 21, no. S3, 2013."

[13] Z. Feng, L. Huang, M. Gong, and G. Jin, "Beam shaping system design using double freeform optical surfaces," *Optics Express*, vol. 21, no. 12, p. 14728, 2013.

[14] D. Sabui, S. Chatterjee, A. Prakash, B. Roy, and G. S. Khan, "Design of an off-axis freeform diversity receiver to improve SINR performance of a multi-cell VLC system," *Optics Communications*, p. 127937, 2022.

[15] J. Garcia and C. Valencia-Estrada, "Freeform compound concentrators for indoor optical wireless communications," *Nonimaging Optics: Efficient Design for Illumination and Solar Concentration XVII*, 2020.

[16] D. A. Bykov, L. L. Doskolovich, A. A. Mingazov, E. A. Bezus, and N. L. Kazanskiy, "Linear assignment problem in the design of freeform refractive optical elements generating prescribed irradiance distributions," *Optics Express*, vol. 26, no. 21, p. 27812, 2018.

[17] "Si APD S12023-02 — Hamamatsu Photonics," www.hamamatsu.com. https://www.hamamatsu.com/eu/en/product/optical-sensors/apd/si-apd/S12023-02.html (accessed Nov. 09, 2022).